

# Garvin's Generalized Problem Revisited

By Francisco J. Sánchez-Sesma<sup>1</sup>, Ursula Iturrarán-Viveros<sup>2</sup> and Eduardo Kausel<sup>3</sup>

## Abstract

One of the great classical problems in theoretical seismology is Garvin's problem, which deals with the response of an elastic half-space subjected to a blast line source applied in its interior. However, Garvin (1956) himself provided only the solution for points on the free surface of the half-space. Although a rigorous extension to points in the interior of the half-space was given nearly decade-and-a-half later by Alterman & Loewenthal (1969), these scientists published their paper in a technical journal of rather restricted circulation, as a result of which their complete solution remained largely unnoticed by the geophysical and soil dynamics communities. This article revisits Garvin's generalized problem, presents a concise rendition and summary together with a very effective and accurate simplification, and examines the response characteristics for a pair of buried source-receiver location. It also includes a compact and very effective Matlab program for its evaluation.

## Introduction

Among the handful of emblematic, canonical problems in theoretical seismology is one due to Walter William Garvin, who in 1956 found exact expressions for the vibration signatures elicited by a two-dimensional (i.e. line) blast source buried at an arbitrary depth within a homogeneous and isotropic half-plane. However, Garvin himself limited his formulation to the displacements observed on the surface of the half-plane and —like Fermat's intriguing annotation some three centuries earlier about the margin of his copy of the ancient book *Arithmetica* being too small to contain the wonderful proof to the famous theorem he had found— he stated that “*the method is equally applicable to any interior points and yields results in the same simple form*”. Unfortunately, Garvin's missing proof was neither obvious nor easy to come by, and thus it remained lacking in the decades that followed his publication. Moreover, Garvin himself vanished without a trace from the scientific community only a few years later, for his last known technical contribution seems to have been a 1960 book on *Linear Programming* that he published while working at the *California Research Corporation* in La Habra, CA. At that time this was a research arm of the *Standard Oil Corporation of California*, which after a merger with *Gulf Oil* became the *Chevron Research Company*.

Some thirteen years after Garvin's famous paper in the *Proceedings of the Royal Society of London*, Alterman & Lowenthal reconsidered the topic and supplied in 1969 the missing proof to Garvin's complete problem, but they did so in the *Israel Journal of*

---

<sup>1</sup> Professor, Instituto de Ingeniería, Universidad Nacional Autónoma de México, CU, Coyoacán 04510, Mexico D.F., Mexico.

<sup>2</sup> Researcher, Facultad de Ciencias, Universidad Nacional Autónoma de México, CU, Coyoacán 04510, Mexico D.F., Mexico

<sup>3</sup> Professor, Department of Civil and Environmental Engineering, Massachusetts Institute of Technology, Cambridge Massachusetts, USA

*Technology*, a multi-disciplinary journal of limited international circulation, a situation which caused this valuable contribution to remain virtually unnoticed and unknown within the seismological and wave motion communities to this day. It is the purpose of this paper to revisit and divulge that solution in the context of a modern and transparent rendition, present a very effective simplification together with an analysis of its range of validity, and to examine the characteristics of the motions for a typical combination of source-receiver locations.

In principle Garvin's problem is intimately related to the two-dimensional version of Lamb's classical problem (1904) for a set of four line loads arranged to form a pair of tensile dipoles. Indeed, Garvin's solution at a point can be shown to equal a linear combination of the gradients of the displacements elicited by suddenly applied horizontal and vertical line loads with respect to the position of the source. Regrettably, this rigorous, formal correspondence is of no help to us in finding the analytical expression for Garvin's problem because the solution to Lamb's problem is only known for a source in the interior and receivers placed at the surface of the half-space and vice-versa, yet not for sources and receivers which lie both simultaneously at arbitrary locations in the interior of the half-space. A complete solution to Lamb's problem in three dimensions valid for any arbitrary Poisson's ratio was very recently given by Kausel (2012), but once again only for a source on the surface and receivers which are located either on the free surface or at depth along the epicentral axis. Conceivably, the Alterman-Loewenthal method might in due time allow an extension of Lamb's two-dimensional problem to arbitrary locations of sources and receivers.

### ***Garvin's classical problem***

Consider an elastic half-plane, i.e. a 2-D half-space subjected to a line blast source at some arbitrary depth  $h > 0$ . The pressure characterizing the blast load is a step function (i.e. Heaviside function) in time, and displacements are sought at arbitrary location in the half-plane. The origin of coordinates  $x=0, z=0$  is at the free surface immediately above the source and the vertical axis  $z$  points down into the half-plane and intersects the source. Vertical displacements are also positive down.

Although direct numerical solutions existed for this problem, Garvin obtained a set of *exact*, closed-form, algebraic expressions for the displacements directly as a function of time  $t$  by means of contour integration, which entails deforming the path of integration so that the resulting integral can be solved analytically. In a nutshell, the problem is first formulated in the frequency-horizontal wavenumber domain and the solution in the time domain expressed formally in terms of a double inverse Laplace transform into time and space. The latter is then cast in terms of a contour integral whose path is cleverly deformed so that the integrand of the double transform reduces to a form with a known transform, in which case the inversion ensues without much ado by direct inspection. This powerful strategy has been widely used and is commonly referred to as the *Cagniard-de Hoop* method, in honor of their inventors (De Hoop, 1960). After this is done, the response functions at the surface are found to be given by the following expressions (see Kausel, 2006, but appropriately modified to account for the different sign convention employed herein for the vertical direction):

$$u_x(x, 0, t, h) = \frac{1}{\pi\mu r} \operatorname{Im} \left\{ \frac{2q_\alpha \sqrt{1+q_\alpha^2}}{R(q_\alpha^2)} \frac{\partial q_\alpha}{\partial \tau} \right\} \operatorname{sgn}(x) \mathcal{H}(\tau - a) \quad (1a)$$

$$u_z(x, 0, t, h) = \frac{-1}{\pi\mu r} \operatorname{Re} \left\{ \frac{(1+2q_\alpha^2)}{R(q_\alpha^2)} \frac{\partial q_\alpha}{\partial \tau} \right\} \mathcal{H}(\tau - a) \quad (1b)$$

where  $\mathcal{H}(\tau - a)$  is the Heaviside (i.e. unit step) function and

$$R(q_\alpha^2) = (1+2q_\alpha^2)^2 - 4q_\alpha^2 \sqrt{q_\alpha^2 + a^2} \sqrt{q_\alpha^2 + 1} = \text{Rayleigh function} \quad (2a)$$

$$q_\alpha = i\tau \sin \theta_z + \cos \theta_z \sqrt{\tau^2 - a^2}, \quad \frac{\partial q_\alpha}{\partial \tau} = i \sin \theta_z + \frac{\tau \cos \theta_z}{\sqrt{\tau^2 - a^2}} = \frac{\sqrt{q_\alpha^2 + a^2}}{\sqrt{\tau^2 - a^2}} \quad (2b)$$

$$\tau = \frac{\beta t}{r}, \quad \sin \theta_z = \frac{|x|}{r}, \quad \cos \theta_z = \frac{h}{r}, \quad r = \sqrt{x^2 + h^2}, \quad a = \frac{\beta}{\alpha} = \sqrt{\frac{1-2\nu}{2(1-\nu)}} \quad (2c)$$

These parameters must satisfy  $\operatorname{Re} q_\alpha \geq 0$ ,  $\operatorname{Re} \sqrt{q_\alpha^2 + a^2} \geq 0$ ,  $\operatorname{Re} \sqrt{q_\alpha^2 + 1} \geq 0$ ,  $\operatorname{Im} \sqrt{\tau^2 - a^2} \leq 0$ , and  $\operatorname{Im} \sqrt{\tau^2 - 1} \leq 0$ , that is, the terms involving square roots in time must have a negative imaginary part when  $\tau$  is small. Observe from eq. 2b that the function  $q_\alpha$  is known *explicitly* in terms of time.

At long times, the displacements tend asymptotically to their static values. Evaluation of this limit when  $\tau \rightarrow \infty$  implies in turn  $q_\alpha \rightarrow \infty$ , which results in the following trends:

$$\lim_{q_\alpha \rightarrow \infty} R(q_\alpha^2) \rightarrow \frac{1}{1-\nu} q_\alpha^2, \quad \lim_{q_\alpha \rightarrow \infty} \sqrt{1+q_\alpha^2} \rightarrow q_\alpha, \quad \lim_{q_\alpha \rightarrow \infty} \frac{\partial q_\alpha}{\partial \tau} = e^{i\theta_z}$$

so

$$\begin{aligned} u_x(x, 0, \infty) &= \frac{1}{\pi\mu r} \lim_{q_\alpha} \left[ \operatorname{Im} \left\{ \frac{2q_\alpha \sqrt{1+q_\alpha^2}}{R(q_\alpha^2)} \frac{\partial q_\alpha}{\partial \tau} \right\} \right] \operatorname{sgn}(x) \\ &= \frac{1}{\pi\mu r} \operatorname{Im} (2(1-\nu) e^{i\theta_z}) \operatorname{sgn}(x) \\ &= \frac{2(1-\nu)}{\pi\mu r} \sin \theta_z \operatorname{sgn}(x) \end{aligned} \quad (3a)$$

Similarly,

$$u_z(x, 0, \infty) = -\frac{2(1-\nu)}{\pi\mu r} \cos \theta_z, \quad (3b)$$

as also given by Kausel (2006).

## Alterman-Loewenthal extension to interior points

Zipora Alterman (1925-1974) and Dan Loewenthal (1943-2000) —henceforth referred to as A&L for short— were both Professors of Geophysics at Tel Aviv University, and both passed away at the relatively young ages of 49 and 57 years, respectively. Although they had found an *exact* solution to a remarkable problem in elastodynamics, they chose as venue for their publication a relatively obscure multidisciplinary journal, as a result of which their contribution remained largely unnoticed by the cognoscenti. Moreover, in typical fashion of many papers in applied mathematics, their presentation was rather terse and sketchy, and they left to the readers the task of distilling the important details out of the formulation and deciphering how the various parts of the solution ultimately fit together. In the ensuing, we omit altogether the mathematical details, which can be found in A&L, and provide instead a synthesis of the most important formulas for the displacement components in a form that is easy to understand and implement.

### a) Travel times

Consider an elastic, homogeneous half-space within which a suddenly applied, dilatational line source acts at the point  $(0, h)$ , which gives rise to a wave field that is observed at a receiver at some arbitrary location  $(x, z)$ , see Fig. 1. Allow also for an image source to be placed symmetrically above the surface of the half-space, and define the radial distances  $r_1, r_2$  and angles of inclination  $\theta_1, \theta_2$  with respect to the vertical as follows:

$$r_1 = \sqrt{x^2 + (z - h)^2}, \quad r_2 = \sqrt{x^2 + (z + h)^2} \quad (4a)$$

$$\sin \theta_1 = \frac{x}{r_1}, \quad \cos \theta_1 = \frac{z - h}{r_1} \quad (4b)$$

$$\sin \theta_2 = \frac{x}{r_2}, \quad \cos \theta_2 = \frac{z + h}{r_2} \quad (4c)$$

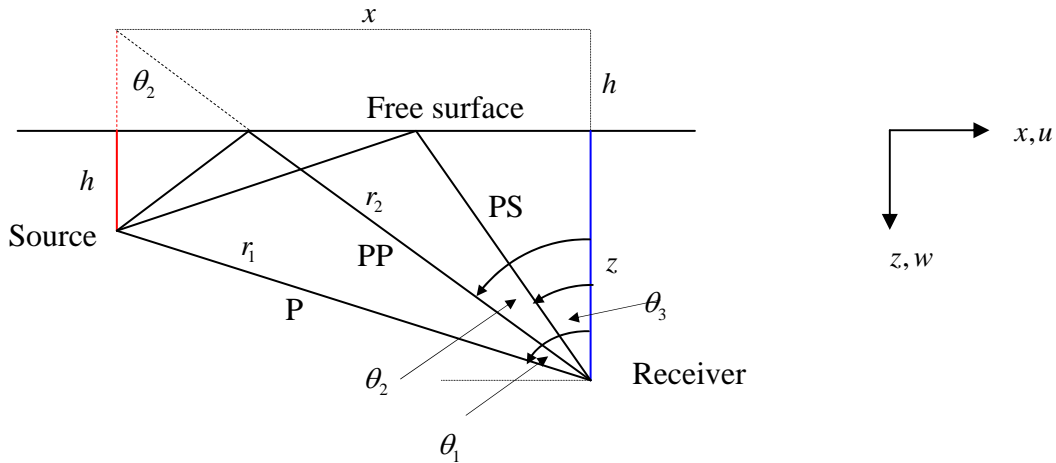


**Figure 1:** Reflection of rays at surface of half-space

The ray  $r_1$  from the source defines the path of the direct P wave, while  $r_2$  represents the distance traveled by the PP ray originating at the image source, and therefore, the distance traveled by the P ray which reflects as a PP wave at the surface. Thus, if  $\alpha$  is the speed of dilatational waves, the characteristic travel times of waves along these two rays are simply

$$t_p = \frac{r_1}{\alpha} \quad \text{and} \quad t_{pp} = \frac{r_2}{\alpha} \quad (5)$$

It can further be shown that of all PP waves with cylindrical wave fronts diffracted at the surface and passing through the receiver, the PP wave associated with the direct ray from the image point has the shortest travel time.

On the other hand, as the P waves impinge on the surface, they also convert partially to shear (or PS) waves as they reflect at various points on the surface in their indirect way to the receiver. Of these converted waves, there exists one pair of P–PS rays which exhibit the shortest travel time, and that pair is the one that satisfies Snell's law. Let  $\theta_p, \theta_s$  be the angles with respect to the vertical which that P–PS pair of rays form at the surface (observe that  $\theta_s = \theta_3$  in Fig. 1 ). Hence

$$x = h \tan \theta_p + z \tan \theta_s \quad (6)$$

$$\frac{\sin \theta_s}{\sin \theta_p} = \frac{\beta}{\alpha} \quad (\text{Snell's law}) \quad (7)$$

for which the minimum travel time is

$$t_{ps} = \frac{h}{\alpha \cos \theta_p} + \frac{z}{\beta \cos \theta_s} \quad (8)$$

Elimination of the terms in the incidence and reflection angles  $\theta_p, \theta_s$  between equations 6-8 is cumbersome and leads to a complicated equation. Nonetheless, a straightforward and highly accurate iterative solution is easily obtained by searching for the point in the interval  $[x_p, x]$  that satisfies Snell's relationship, where  $x_p$  is the intersection of the PP ray with the free surface. Thus,  $t_{ps}$  can readily be determined to high accuracy, and can thus be assumed to be known.

In the ensuing, we find it convenient to make use of dimensionless parameters, which we achieve by normalizing the time variable as follows:

$$\tau = \frac{t\beta}{r_2} \quad (9)$$

where  $\beta$  is the shear wave velocity and  $r_2$  is the distance from the image point to the receiver. Hence, the dimensionless travel times are

$$\tau_P = \frac{t_P \beta}{r_2} = \frac{r_1}{r_2} \frac{\beta}{\alpha} = \frac{r_1}{r_2} a, \quad a = \frac{\beta}{\alpha} = \sqrt{\frac{1-2\nu}{2(1-\nu)}} \quad (10a)$$

$$\tau_{PP} = \frac{t_{PP} \beta}{r_2} = \frac{\beta}{\alpha} = a \quad (10b)$$

$$\tau_{PS} = \frac{t_{PS} \beta}{r_2} \quad (10c)$$

### ***b) Cagniard-DeHoop paths***

As mentioned earlier, when the primary waves emitted by the source impinge upon the surface, they reflect as PP and PS waves, and they also convert in part into Rayleigh waves. As shown by A&L, a detailed analysis of the interaction of these various wave components leads to a pair of integrals associated with the PP and PS waves which can be evaluated in closed form by means of the well-known Cagniard-DeHoop technique. This involves deforming the integration path in the complex plane so as to achieve an integrand whose inverse Laplace transform can be found by simple inspection. Expressed in dimensionless time, these two paths are

$$\tau \equiv \tau_{\alpha\alpha} = \cos \theta_2 \sqrt{q_{\alpha\alpha}^2 + a^2} - i q_{\alpha\alpha} \sin \theta_2, \quad \tau_{\alpha\alpha} \geq \tau_{PP} \quad (11a)$$

$$\tau \equiv \tau_{\alpha\beta} = H \sqrt{q_{\alpha\beta}^2 + a^2} + Z \sqrt{q_{\alpha\beta}^2 + 1} - i X q_{\alpha\beta} \quad \tau_{\alpha\beta} \geq \tau_{PS} \quad (11b)$$

$$H = \frac{h}{r_2}, \quad Z = \frac{z}{r_2}, \quad X = \frac{x}{r_2} \quad (11c)$$

where  $q_{\alpha\alpha}, q_{\alpha\beta}$  are dimensionless, complex-valued auxiliary functions constrained in such a way that  $\tau_{\alpha\alpha}, \tau_{\alpha\beta}$  must remain real. They must satisfy

$$\operatorname{Re} q_{\alpha\alpha} \geq 0, \quad \operatorname{Re} \sqrt{q_{\alpha\alpha}^2 + a^2} \geq 0, \quad \operatorname{Re} \sqrt{q_{\alpha\alpha}^2 + 1} > 0 \quad (12a)$$

$$\operatorname{Re} q_{\alpha\beta} \geq 0, \quad \operatorname{Re} \sqrt{q_{\alpha\beta}^2 + a^2} \geq 0, \quad \operatorname{Re} \sqrt{q_{\alpha\beta}^2 + 1} > 0 \quad (12b)$$

Their derivatives, which are also needed, can be shown to be given by

$$\begin{aligned} \frac{\partial q_{\alpha\alpha}}{\partial \tau} &= \frac{\tau}{\sqrt{\tau^2 - a^2}} \cos \theta_2 + i \sin \theta_2 \\ &= \left[ \frac{q_{\alpha\alpha}}{\sqrt{q_{\alpha\alpha}^2 + a^2}} \cos \theta_2 - i \sin \theta_2 \right]^{-1} \end{aligned} \quad (13a)$$

$$\frac{dq_{\alpha\beta}}{d\tau} = \left[ \left( \frac{q_{\alpha\beta}}{\sqrt{q_{\alpha\beta}^2 + a^2}} H + \frac{q_{\alpha\beta}}{\sqrt{q_{\alpha\beta}^2 + 1}} Z \right) - i X \right]^{-1} \quad (13b)$$

Evaluation of the integrals requires an inversion of eqs. 11a,b into the form  $q_{\alpha\alpha} = q_{\alpha\alpha}(\tau)$  and  $q_{\alpha\beta} = q_{\alpha\beta}(\tau)$ . The first is readily obtained by solving for  $q_{\alpha\alpha}$  from the quadratic equation inferred from eq. 11a,

$$(\tau + i q_{\alpha\alpha} \sin \theta_2)^2 = (q_{\alpha\alpha}^2 + a^2) \cos^2 \theta_2 \quad (14)$$

which yields two inverses, of which only one has a positive real part, namely

$$q_{\alpha\alpha}(\tau) = \cos \theta_2 \sqrt{\tau^2 - a^2} + i \tau \sin \theta_2 \quad (15)$$

which agrees with eq. 2b. On the other hand, and as shown in Appendix I, elimination of the square root terms in eq. 11b leads to the quartic equation in  $q \equiv q_{\alpha\beta}(\tau)$ , with  $\tau \equiv \tau_{\alpha\beta}$ :

$$Aq^4 - 4iBq^3 - 2Cq^2 + 4iDq + E = 0 \quad (16)$$

with all *real* coefficients

$$A = \left[ (H + Z)^2 + X^2 \right] \left[ (H - Z)^2 + X^2 \right] > 0 \quad (17a)$$

$$B = \tau X (H^2 + X^2 + Z^2) > 0 \quad (17b)$$

$$C = \tau^2 (H^2 + 3X^2 + Z^2) - \left[ X^2 (H^2 a^2 + Z^2) + (H^2 - Z^2) (H^2 a^2 - Z^2) \right] \quad (17c)$$

$$D = \tau X \left[ \tau^2 - (H^2 a^2 + Z^2) \right] \quad (17d)$$

$$E = \left( \tau^2 - (Ha + Z)^2 \right) \left( \tau^2 - (Ha - Z)^2 \right) \quad (17e)$$

This quartic equation admits four roots which can appear in one of the following alternative forms (further details together with an example and a figure showing the roots are given in Appendix I):

- a) All roots are complex and appear in negative complex conjugate pairs (this is the norm when  $\tau > \tau_{PS}$ ):  
 $q_1, q_2, q_3 = -q_1^*, q_4 = -q_2^*$
- b) There exists one pair of negative complex conjugate roots and two distinct, purely imaginary roots:  
 $q_1, q_2 = -q_1^*, q_3 = iQ_3, q_4 = iQ_4$ , (with  $Q_3, Q_4$  being real quantities)
- c) There are four distinct, purely imaginary roots:  
 $q_1 = iQ_1, q_2 = iQ_2, q_3 = iQ_3, q_4 = iQ_4$ , (All  $Q_j$  are real quantities)
- d) No purely real roots can exist.

When the four solutions for the case at hand are plotted in term of dimensionless time, it is found that they consist of four branches, two of which have negative real parts and can thus be discarded on account of (12b). Of the remaining two roots, it is shown in Appendix I that at least one of these two roots is *guaranteed* to have a positive imaginary part, and possibly even both roots have such a characteristic. Either way, we choose the one with the smallest *positive* imaginary part, which is also the sole branch which starts as a purely imaginary, positive root when  $\tau = \tau_{PS}$ , i.e. at the arrival of the PS waves at the receiver, in agreement with ray theory. The rejection of the second root can be further justified by observing that it would introduce non-physical singularities as well as non-causal arrivals.

In principle, the quartic equation (16) could be evaluated in closed form by means of Ferrari's classical formula. However, a more convenient and robust alternative is to rely on a numerical routine for the roots of polynomials such as the "roots" function in Matlab, which although conceptually slower than Ferrari's, its slowness is irrelevant because in an actual problem the execution time required proves to be negligible.

### c) Displacements at the receiver

Assuming that we have accomplished the inversion of  $q_{\alpha\alpha}(\tau), q_{\alpha\beta}(\tau)$  together with their derivatives  $\partial q_{\alpha\alpha}/\partial\tau, \partial q_{\alpha\beta}/\partial\tau$ , we proceed to use these to evaluate the Rayleigh functions

$$R_{\alpha\alpha}(\tau) = \left(1 + 2q_{\alpha\alpha}^2\right)^2 - 4q_{\alpha\alpha}^2 \sqrt{1 + q_{\alpha\alpha}^2} \sqrt{a^2 + q_{\alpha\alpha}^2} \quad (18a)$$

$$R_{\alpha\beta}(\tau) = \left(1 + 2q_{\alpha\beta}^2\right)^2 - 4q_{\alpha\beta}^2 \sqrt{1 + q_{\alpha\beta}^2} \sqrt{a^2 + q_{\alpha\beta}^2} \quad (18b)$$

Distilling from A&L the final results of the four contour integrals which arise in the Cagniard-De Hoop method, we obtain the following displacements:

#### Horizontal displacement:

$$u = \frac{1}{\pi\mu} \left\{ \frac{1}{2r_1} \frac{\tau}{\sqrt{\tau^2 - \tau_p^2}} \sin\theta_1 \mathcal{H}(\tau - \tau_p) - \frac{1}{2r_2} \frac{\tau}{\sqrt{\tau^2 - \tau_{PP}^2}} \sin\theta_2 \mathcal{H}(\tau - \tau_{PP}) \right. \\ \left. - \frac{4}{r_2} \operatorname{Im} \left[ \frac{q_{\alpha\alpha}^3 \sqrt{q_{\alpha\alpha}^2 + 1}}{R_{\alpha\alpha}} \frac{\partial q_{\alpha\alpha}}{\partial\tau} \right] \mathcal{H}(\tau - \tau_{PP}) + \frac{2}{r_2} \operatorname{Im} \left[ \frac{q_{\alpha\beta} (1 + 2q_{\alpha\beta}^2) \sqrt{1 + q_{\alpha\beta}^2}}{R_{\alpha\beta}} \frac{\partial q_{\alpha\beta}}{\partial\tau} \right] \mathcal{H}(\tau - \tau_{PS}) \right\} \quad (19a)$$

#### Vertical displacement

$$w = \frac{1}{\pi\mu} \left\{ \frac{1}{2r_1} \frac{\tau}{\sqrt{\tau^2 - \tau_p^2}} \cos\theta_1 \mathcal{H}(\tau - \tau_p) + \frac{1}{2r_2} \frac{\tau}{\sqrt{\tau^2 - \tau_{PP}^2}} \cos\theta_2 \mathcal{H}(\tau - \tau_{PP}) \right. \\ \left. - \frac{1}{r_2} \operatorname{Re} \left[ \frac{(1 + 2q_{\alpha\alpha}^2)^2}{R_{\alpha\alpha}} \frac{\partial q_{\alpha\alpha}}{\partial\tau} \right] \mathcal{H}(\tau - \tau_{PP}) + \frac{1}{r_2} \operatorname{Re} \left[ \frac{2q_{\alpha\beta}^2 (1 + 2q_{\alpha\beta}^2)}{R_{\alpha\beta}} \frac{\partial q_{\alpha\beta}}{\partial\tau} \right] \mathcal{H}(\tau - \tau_{PS}) \right\} \quad (19b)$$



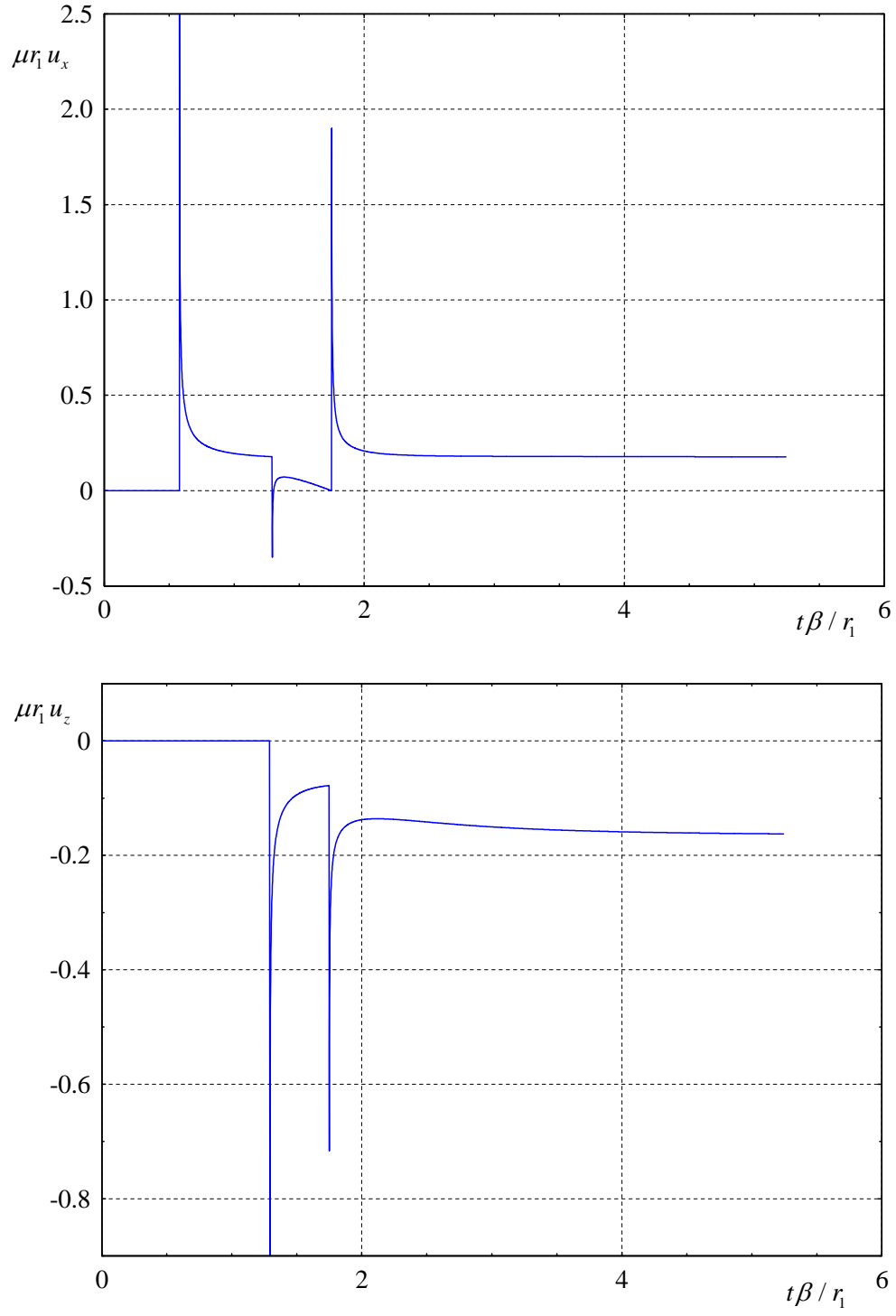


**Figure 2a,b:** Response function for a source at depth  $h=1$  observed at a receiver at location  $x=1, z=1$  for Poisson's ratio  $\nu=0.25$

where  $\tau, \tau_p, \tau_{pp}, \tau_{ps}$  are defined by equations 9, 10a-c;  $q_{\alpha\alpha}(\tau), q_{\alpha\beta}(\tau)$  are given by eqs. 15 together with the numerical solution to eq. 16; also, the partial derivatives are given by 13a,b. Figures 2a, 2b show the horizontal and vertical displacements for a source-receiver combination  $z = h = z = 1$  and material parameters  $\beta = 1, \nu = 0.25$ , which corresponds to Lamé parameters  $\mu = \lambda = 1$ . For convenience, we have chosen to display the time axis normalized with respect to  $r_1$ . The three peaks in the horizontal response correspond to the arrivals of the P, PP and PS waves. The vertical response shows only two peaks because the direct P wave travels horizontally from the source to the receiver, and thus has no vertical components.

#### d) Asymptotic(static) behavior

As time increases, the displacements approach their static values. These can be obtained from the limits: [Error found after publication: See CORRIGENDUM on page 25]

$$q_{\alpha j} \rightarrow \tau e^{i\theta_2}, \quad \frac{\partial q_{\alpha j}}{\partial \tau} \rightarrow e^{i\theta_2}, \quad R_{\alpha j} \rightarrow 2(1-a^2)q_{\alpha j}^2 = \frac{1}{1-\nu}q_{\alpha j}^2, \quad j = \alpha, \beta$$

so

$$\begin{aligned} u &= \frac{1}{\pi\mu} \left[ \frac{1}{2r_1} \sin \theta_1 - \frac{1}{2r_2} \sin \theta_2 + \frac{2(1-\nu)}{r_2} \sin \theta_2 \right] \\ &= \frac{1}{2\pi\mu} \left[ \frac{1}{r_1} \sin \theta_1 + \frac{3-4\nu}{r_2} \sin \theta_2 \right] \end{aligned} \quad (20a)$$

$$\begin{aligned} w &= \frac{1}{\pi\mu} \left\{ \frac{1}{2r_1} \cos \theta_1 + \frac{1}{2r_2} \cos \theta_2 - \frac{2(1-\nu)}{r_2} \cos \theta_2 \right\} \\ &= \frac{1}{2\pi\mu} \left\{ \frac{1}{r_1} \cos \theta_1 - \frac{3-4\nu}{r_2} \cos \theta_2 \right\} \end{aligned} \quad (20b)$$

### Approximate solution

Inasmuch as we have just summarized the formulas for the full, exact solution to Garvin's generalized problem and that they do not take a convoluted form, it might seem peculiar that we may also wish to provide an approximate solution, but there are good reasons for this. As can be seen from eqs. 19a,b, the full solution is given in terms of the function  $q_{\alpha\beta}(\tau)$  that is not known in explicit form, but which must be obtained from the numerical solution to a quartic equation and chosen appropriately from its four solutions, as explained earlier. As it turns out, an excellent, *explicit* functional approximation to that inversion can be obtained, which not only is attractive in its own right, but also provides insight into the problem at hand.

As seen earlier, the Cagniard-De Hoop path for PS waves is defined by (eqs. 11b,c):

$$\tau_{\alpha\beta} = H \sqrt{q_{\alpha\beta}^2 + a^2} + Z \sqrt{q_{\alpha\beta}^2 + 1} - i X q_{\alpha\beta} \quad \tau_{\alpha\beta} \geq \tau_{ps} \quad (21a)$$

$$H = \frac{h}{r_2}, \quad Z = \frac{z}{r_2}, \quad X = \frac{x}{r_2} \quad (21b)$$

A close approximation to the above paths is given by

$$\begin{aligned} \tau_{app} &= H_{eq} \sqrt{q_{app}^2 + a^2} - i X_{eq} q_{app} \\ &= \cos \theta_{eq} \sqrt{q_{app}^2 + a^2} - i q_{app} \sin \theta_{eq} \end{aligned} \quad (22a)$$

where

$$H_{eq} = \frac{h_{eq}}{r_{eq}}, \quad X_{eq} = \frac{x_{eq}}{r_{eq}}, \quad (23a)$$

$$h_{eq} = h + z / a, \quad x_{eq} = \frac{h + z / a}{h + z} x \quad (23b)$$

$$r_{eq} = \sqrt{h_{eq}^2 + x_{eq}^2} = \frac{h + z / a}{h + z} r_2 \quad (23c)$$

$$\cos \theta_{eq} = \frac{h_{eq}}{r_{eq}}, \quad \sin \theta_{eq} = \frac{x_{eq}}{r_{eq}} \quad (23d)$$

in terms of which

$$q_{app} = \frac{h + z}{h + z / a} q_{\alpha\beta} \quad (24)$$

The approximation (22a) has exactly the same form as  $\tau_{\alpha\alpha}$  in Garvin's solution, so its explicit inverse is

$$\begin{aligned} q_{app} &= \cos \theta_{eq} \sqrt{\tau_{app}^2 - a^2} + i \tau_{app} \sin \theta_{eq} \\ &= \cos \theta_2 \sqrt{\tau_{app}^2 - a^2} + i \tau_{app} \sin \theta_2 \end{aligned} \quad (25)$$

From eqs. 24, 25, it then follows that

$$q_{\alpha\beta} \approx \frac{r_{eq}}{r_2} \left( \cos \theta_2 \sqrt{\tau_{app}^2 - a^2} + i \tau_{app} \sin \theta_2 \right) \quad (26)$$

where

$$\tau_{app} = \frac{t\beta}{r_{eq}} = \frac{t\beta}{r_2} \frac{r_2}{r_{eq}} = \frac{h + z}{h + z / a} \tau_2, \quad t > t_{PS} \quad (27)$$

On the other hand, from (13b) as well as the preceding equations, we have

$$\frac{dq_{\alpha\beta}}{d\tau} = \left[ \frac{q_{\alpha\beta}}{\sqrt{q_{\alpha\beta}^2 + a^2}} \frac{h}{r_{eq}} + \frac{q_{\alpha\beta}}{\sqrt{q_{\alpha\beta}^2 + 1}} \frac{z}{r_{eq}} - i \frac{x}{r_{eq}} \right]^{-1} \quad (28)$$

With 26 and 28, we have now all of the instruments needed to evaluate explicitly the last term in the displacement equations 19a,b. Observe that in this approximation, the  $q_{\alpha\beta}$  function given by (26) is simply a time-stretched, scaled replica of the  $q_{\alpha\alpha}$  function, i.e. of the PP reflection.

Figure 3 shows a comparison of the exact inversion of the quartic equation vs. the approximation given by eq. 26, as function of dimensionless time, for the same data considered earlier, i.e. a source at  $h=1$  and a receiver at  $x=z=1$  for Poisson's ratio  $\nu=0.25$  and Lamé parameters  $\lambda=\mu=1$ . As can be seen, the approximation is excellent, and in fact improves further for more distant receivers. An extensive set of additional numerical tests reveal that the approximation works fairly well for other source-receiver distances together with modest values of Poisson's ratio  $\nu$ , but breaks down for high values, say close to or above  $\nu=0.45$ .

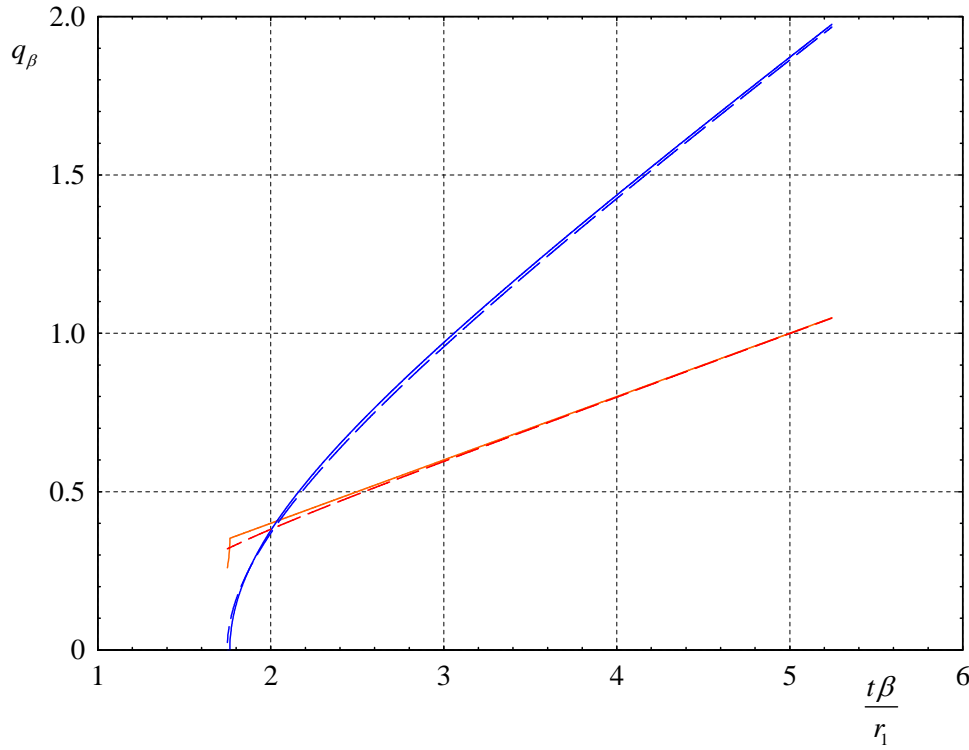


**Figure 3:** Exact inversion of  $q_{\beta}$  vs. approximate inversion via eqs. 26,27.

An implication of this approximation concerns the time of arrival of the PS waves. As explained earlier in connection with the solution to the quartic, this occurs when  $\text{Re}(q_{\alpha\beta})=0$ ,  $\tau_{app} = a = \beta / \alpha$ , which implies  $t_{PS}\beta / r_{eq} = a$ . This leads to the explicit estimation formula,

$$t_{PS} = \left( \frac{h+z/a}{h+z} \right) \frac{r_2}{\alpha} = \frac{h+z/a}{h+z} t_{PP} = \left( \frac{h}{\alpha} + \frac{z}{\beta} \right) \frac{1}{\cos \theta_2} \quad (28)$$

Numerical tests demonstrate that the estimation for the time of arrival of PS waves works well. Observe that  $h/\alpha/\cos \theta_2$  is the travel time of P waves to the surface along the incident PS ray and  $z/\beta/\cos \theta_2$  is the travel time of S waves from the surface to the receiver along the reflected PP ray.

## **Conclusions**

Alterman & Lowenthal 1969 extension to Garvin's problem of a blast line source acting within an elastic, homogeneous and isotropic half-space undoubtedly constitutes a major advance in theoretical seismology, even if it remained dormant for some four decades. Unlike Garvin's classical solution, it is not restricted to receivers on the free-surface, but allows computing motion signatures which are rich in all frequencies and then again at arbitrary points within the half-space. Thus, it is the ideal tool to be used as a benchmark for the validation of numerical solutions obtained with finite elements (or finite differences) augmented with numerical devices such as transmitting boundaries or perfectly matched layers.

In the preceding pages we provided a succinct account of this emblematic problem, summarized the final exact solution for the signatures at arbitrary receivers, and discussed in general terms the details of the quartic equation needed for the inversion of the Cagniard-DeHoop path associated with PS waves. A brief Matlab program included as an appendix allows not only obtaining theoretical seismograms in digital and graphic form for any arbitrary pair of source and receiver locations, but can also be used as a resource to discern the details and attain a deeper understanding of the fundamental elements of the solution.

Finally, we devised and presented a close approximation to the quartic root which not only provides further insight into the problem but which opens the door to obtain integrated versions of the displacements by convolution with any source function. This could be used in turn as an additional benchmark for the testing of numerical methods, even if it should require further development and testing in papers yet to be written.

## **Acknowledgements**

We dedicate this article to our most esteemed colleague and friend, Professor José Manuel Roësset. His many contributions to education and engineering science, not to mention his charm, elegance and deep knowledge are among the virtues we cherish most.

We are also grateful to Caltech Prof. Emer. Hiroo Kanamori for bringing to our attention a paper by Murrell & Ungar (1982) which made reference to Alterman & Loewenthal's and in turn made us aware of this pioneering contribution.

This work was partially supported by DGAPA-UNAM under projects IN104712 and IC100511.

## References

- Alterman, Z.S., and Loewenthal, D. (1969). Algebraic expressions for the impulsive motion of an elastic half-space, *Israel Journal of Technology*, **7** (6), 495-504.
- Cagniard, L. (1939). Reflexion et refraction des ondes seismiques progressives. Paris: *Gauthier-Villars*.
- De Hoop, A.T. (1960). A modification of Cagniard's method for solving seismic pulse problems. *Applied Science Research, Section B*, **8**, 349–356.
- Garvin, W.W. (1956). Exact transient solution of the buried line source problem. *Proceedings of the Royal Society of London, Series A*, 528-541.
- Kausel, E. (2006). *Fundamental solutions in elastodynamics. A Compendium*. Cambridge University Press, New York.
- Kausel, E. (2012). Lamb's problem at its simplest. *Proceedings of the Royal Society, Series A*, London, RSPA-20120462.
- Lamb, H. (1904). On the propagation of tremors over the surface of an elastic solid. *Philosophical Transactions of the Royal Society of London, Series A*, **203**, 1–42.
- Murrell H.C. and A. Ungar. (1982) From Cagniard's method for solving seismic pulse problems to the method of the Differential Transform. *Comp. & Math. with Appls.* **8**(2), 103-119
- Sánchez-Sesma, F., and Iturrarán-Viveros, U. (2006): The classic Garvin's problem revisited, *Bulletin of the Seismological Society of America*, **96** (4A), 1344–1351 (August).

## Appendix 1: Solution to quartic equation

With the definitions  $H = h / r$ ,  $Z = z / r$ ,  $X = x / r$ ,  $q \equiv q_{\alpha\beta}$  and  $r$  being an arbitrary scaling length, we can write the Cagniard-deHoop path in dimensionless time  $\tau \equiv \tau_{\alpha\beta}$  (eq. 11b) as

$$\tau = H\sqrt{q^2 + a^2} + Z\sqrt{q^2 + 1} - iXq, \quad \tau = \frac{t\beta}{r}, a = \frac{\beta}{\alpha}$$

so

$$\begin{aligned} (\tau + iXq)^2 &= \left( H\sqrt{q^2 + a^2} + Z\sqrt{q^2 + 1} \right)^2 \\ &= (H^2 + Z^2)q^2 + (H^2a^2 + Z^2) + 2HZ\sqrt{q^2 + a^2}\sqrt{q^2 + 1} \end{aligned}$$

that is

$$\left\{ (\tau + iXq)^2 - \left[ (H^2 + Z^2)q^2 + (H^2a^2 + Z^2) \right] \right\}^2 = 4H^2Z^2(q^2 + a^2)(q^2 + 1)$$

This leads to the quartic equation

$$\begin{aligned} &\left[ (H + Z)^2 + X^2 \right] \left[ (H - Z)^2 + X^2 \right] q^4 - 4i\tau X (H^2 + X^2 + Z^2) q^3 \\ &- 2 \left[ \tau^2 (H^2 + 3X^2 + Z^2) - X^2 (H^2a^2 + Z^2) - (H^2 - Z^2) (H^2a^2 - Z^2) \right] q^2 + 4i\tau X \left[ \tau^2 - (H^2a^2 + Z^2) \right] q \\ &+ \left( \tau^2 - (Ha + Z)^2 \right) \left( \tau^2 - (Ha - Z)^2 \right) = 0 \end{aligned}$$

or

$$\boxed{Aq^4 - 4iBq^3 - 2Cq^2 + 4iDq + E = 0} \quad (29)$$

with all *real* coefficients

$$\boxed{A = \left[ (H + Z)^2 + X^2 \right] \left[ (H - Z)^2 + X^2 \right] > 0} \quad (30a)$$

$$\boxed{B = \tau X (H^2 + X^2 + Z^2) > 0} \quad (30b)$$

$$\boxed{C = \tau^2 (H^2 + 3X^2 + Z^2) - \left[ X^2 (H^2 a^2 + Z^2) + (H^2 - Z^2) (H^2 a^2 - Z^2) \right]} \quad (30c)$$

$$\boxed{D = \tau X \left[ \tau^2 - (H^2 a^2 + Z^2) \right]} \quad (30d)$$

$$\boxed{E = \left( \tau^2 - (Ha + Z)^2 \right) \left( \tau^2 - (Ha - Z)^2 \right)} \quad (30e)$$

Observe that  $A > 0, B > 0$  are always true. Also,  $E = 0$  at  $t = h / \alpha + z / \beta$  before the arrival of the PS wave, at which point in time there exists one root which vanishes altogether. However, for times *after* the arrival of the PS wave  $t \geq t_{ps}$ , both  $D > 0$  and  $E > 0$  because  $t > h / \alpha + z / \beta > \sqrt{h^2 / \alpha^2 + z^2 / \beta^2}$ , or equivalently,  $\tau > \sqrt{H^2 a^2 + Z^2}$ ; in addition,  $t > |h / \alpha + z / \beta| > |h / \alpha - z / \beta|$ , which is the same as  $\tau > |Ha + Z| > |Ha - Z|$ . These conditions imply in turn that  $q = 0$  *cannot* be a solution to the quartic *after* the arrival of the PS wave. Also, in most cases *real* solutions cannot exist either, because these would demand the simultaneous satisfaction of

$$\begin{aligned} Aq^4 - 2Cq^2 + E = 0 & \rightarrow q^2 = \frac{C}{A} \pm \sqrt{\left(\frac{C}{A}\right)^2 - \frac{E}{A}} \\ -Bq^3 + Dq = 0 & \rightarrow q^2 = \frac{D}{B} \end{aligned}$$

Hence, we conclude that all four solutions must be either complex, purely imaginary or a combination of these two.

The structure of the quartic equation is such that if  $q$  is a *complex* solution, then  $-q^*$  is also a solution. To prove this, assume that  $-q^*$  is indeed a solution, then

$$\begin{aligned} \left[ A(-q^*)^4 - 4iB(-q^*)^3 - 2C(-q^*)^2 + 4i\tau D(-q^*) + E \right]^* &= 0^* = 0 \\ &= \left[ A(q^*)^4 + 4iB(q^*)^3 - 2C(q^*)^2 - 4i\tau D(q^*) + E \right]^* \\ &= Aq^4 - 4iBq^3 - 2Cq^2 + 4iDq + E = 0 \end{aligned}$$

However, if the solution were to be purely imaginary, then  $-q^* = q$  would not be a distinct solution, in which case it must be ruled out —save for exceptional points in time at which repeated roots can occur. The conclusion is that if purely imaginary solutions

$q = iQ$  (with real  $Q$ ) exist, then they must appear in distinct pairs. Hence, the set of four solutions must be of one of the forms

$q_1, q_2, q_3 = -q_1^*, q_4 = -q_2^*$	All four roots are complex
$q_1, q_2 = -q_1^*, q_3 = iQ_3, q_4 = iQ_4$	One complex pair and two imaginary roots
$q_1 = iQ_1, q_2 = iQ_2, q_3 = iQ_3, q_4 = iQ_4$	Four imaginary roots

**a) All complex roots**

This is the normal case. If all roots are complex, then the quartic equation must have the form

$$A(q - q_1)(q + q_1^*)(q - q_2)(q + q_2^*) = 0$$

or

$$\left[ q^2 - (q_1 - q_1^*)q - q_1 q_1^* \right] \left[ q^2 - (q_2 - q_2^*)q - q_2 q_2^* \right] = 0$$

This means that –at least in principle– it should be possible to carry out a decomposition of the quartic into the product of two quadratic equations, but this is no simple feat.

Expanding the above product, we obtain

$$\begin{aligned} q^4 - \left[ (q_1 - q_1^*) + (q_2 - q_2^*) \right] q^3 + \left[ (q_1 - q_1^*)(q_2 - q_2^*) - q_1 q_1^* - q_2 q_2^* \right] q^2 \\ + \left[ q_1 q_1^* (q_2 - q_2^*) + (q_1 - q_1^*) q_2 q_2^* \right] + q_1 q_1^* q_2 q_2^* = 0 \end{aligned}$$

or

$$\begin{aligned} q^4 - 2i \left[ \text{Im}(q_1) + \text{Im}(q_2) \right] q^3 - \left[ 4\text{Im}(q_1)\text{Im}(q_2) + |q_1|^2 + |q_2|^2 \right] q^2 \\ + 2i \left[ |q_1|^2 \text{Im}(q_2) + |q_2|^2 \text{Im}(q_1) \right] q + |q_1|^2 |q_2|^2 = 0 \end{aligned}$$

which implies

$$\boxed{B / A = \frac{1}{2} \left[ \text{Im}(q_1) + \text{Im}(q_2) \right] > 0} \quad (31a)$$

$$\boxed{C / A = \frac{1}{2} \left[ 4\text{Im}(q_1)\text{Im}(q_2) + |q_1|^2 + |q_2|^2 \right]} \quad (31b)$$

$$\boxed{D / A = \frac{1}{2} \left[ |q_1|^2 \text{Im}(q_2) + |q_2|^2 \text{Im}(q_1) \right] > 0} \quad (31c)$$

$$\boxed{E / A = |q_1|^2 |q_2|^2 > 0} \quad (31d)$$

In as much as the ratio  $E / A$  in (31d) is necessarily non-negative, then eq. 30e informs us that this can begin to be possible only from shortly before the arrival of the PS wave, namely the time for a P wave to move straight up combined with the time for an S wave to return straight down, i.e. the exceptional zero root for  $E = 0$  referred to earlier.

Furthermore, this very same condition guarantees also that  $D / A > 0$ , so the inequality in eq. 31c is a consequence of the inequality in eq. 31d. Hence, four complex solutions are only possible after this time. However, this by itself does not rule out the possibility of



either two or four purely imaginary roots when  $\tau > |Ha + Z|$ , it only rules out four complex solutions before this time.

When all roots are complex, they will appear in pairs of the form

$$\begin{aligned} q_1 &= a + ib, & q_2 &= c + id \\ q_3 &= -q_1^* = -a + ib & q_4 &= -q_2^* = -c + id \end{aligned}$$

Without loss of generality, we can readily assume that  $a > 0$ ,  $c > 0$ , while  $b, d$  could be either positive or negative. However, eq. 31a implies

$$b + d > 0$$

Again, without loss of generality we can assume  $b > d$ . Hence, the above relationship can only be satisfied if either

$$b > d > 0 \quad \text{or} \quad b > 0 > d \quad \text{with } b > |d|$$

We conclude that there is at least one, and perhaps even two complex roots whose imaginary part is positive. On the other hand, when all roots are complex, then of the four solutions two will have positive real part and the other two will have negative real part. However, an additional requirement in our case is that

$$\text{Re}(q) > 0, \text{Re}(\sqrt{q^2 + a^2}) > 0, \text{Re}(\sqrt{q^2 + 1}) > 0$$

which we can use to reject two of the four solutions available, namely those with negative real part. Of the two remaining roots, there exists at least one with a positive imaginary part, in which case we choose the one with the smaller imaginary part (i.e. the smallest but still positive imaginary part). The branch for this root is the only one that starts as a purely imaginary root when  $t = t_{PS}$ .

#### **b) One complex pair and two imaginary roots:**

The quartic equation is now of the form

$$A(q - q_1)(q + q_1^*)(q - iQ_3)(q - iQ_4) = 0$$

or

$$\left[ q^2 - 2i\text{Im}(q_1)q - |q_1|^2 \right] \left[ q^2 - i(Q_3 + Q_4)q - Q_3Q_4 \right] = 0$$

i.e.

$$\begin{aligned} q^4 - i[Q_3 + Q_4 + 2\text{Im}(q_1)]q^3 - [Q_3Q_4 + 2\text{Im}(q_1)(Q_3 + Q_4) + |q_1|^2]q^2 \\ + i[2\text{Im}(q_1)Q_3Q_4 + |q_1|^2(Q_3 + Q_4)]q + |q_1|^2 Q_3Q_4 = 0 \end{aligned}$$

so

$$\frac{4B}{A} = Q_3 + Q_4 + 2\text{Im}(q_1) > 0 \quad (32a)$$

$$\frac{C}{A} = \frac{1}{2}(Q_3 Q_4 + |q_1|^2) + \text{Im}(q_1)(Q_3 + Q_4) \quad (32b)$$

$$\frac{4D}{A} = 2\text{Im}(q_1)Q_3 Q_4 + |q_1|^2(Q_3 + Q_4) \quad (32c)$$

$$\frac{E}{A} = |q_1|^2 Q_3 Q_4 \quad (32d)$$

This case characterizes the roots at times *before* the arrival of the PS wave. Moreover, at the very instant of arrival  $t = t_{ps}$  the two imaginary roots coalesce into one double, purely imaginary root  $Q_3 = Q_4$  while  $q_1, q_2 = -q_1^*$  continue to define a pair of complex roots. For  $t > t_{ps}$ , the pair of identical roots mutates into a pair of negative complex conjugate roots, in which case the equations in the previous section apply.

### c) Four purely imaginary roots

The quartic is now of the form

$$A(q - iQ_1)(q - iQ_2)(q - iQ_3)(q - iQ_4) = 0$$

or

$$q^4 - i(Q_1 + Q_2 + Q_3 + Q_4)q^3 - [(Q_1 + Q_2)(Q_3 + Q_4) + Q_1 Q_2 + Q_3 Q_4]q^2 + i[(Q_1 + Q_2)Q_3 Q_4 + (Q_3 + Q_4)Q_1 Q_2]q + Q_1 Q_2 Q_3 Q_4$$

implying

$$\frac{4B}{A} = Q_1 + Q_2 + Q_3 + Q_4 > 0 \quad (33a)$$

$$\frac{2C}{A} = (Q_1 + Q_2)(Q_3 + Q_4) + Q_1 Q_2 + Q_3 Q_4 \quad (33b)$$

$$\frac{4D}{A} = (Q_1 + Q_2)Q_3 Q_4 + (Q_3 + Q_4)Q_1 Q_2 \quad (33c)$$

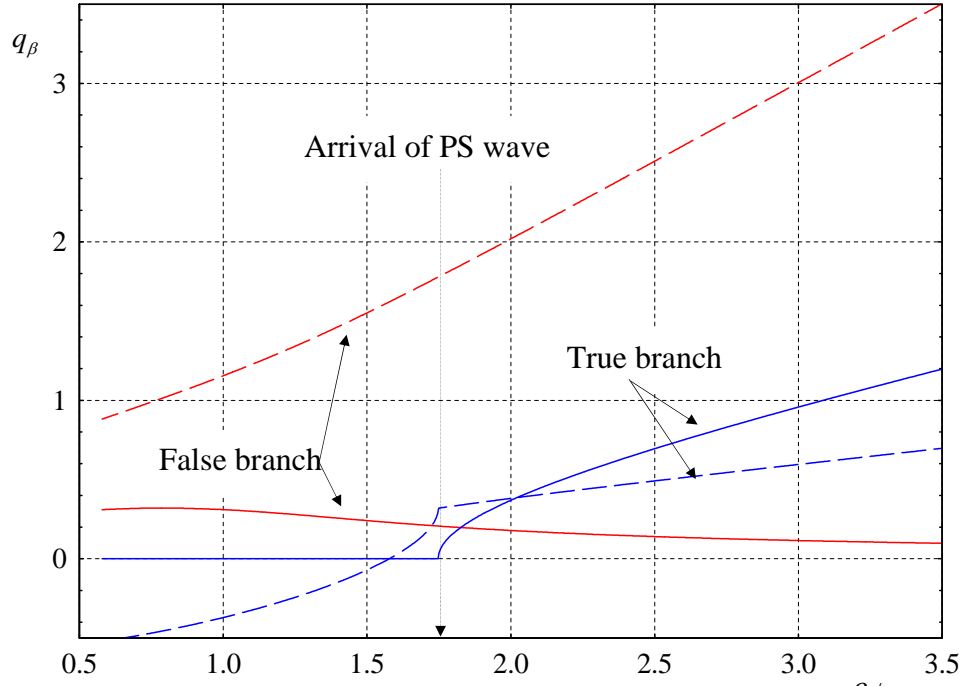
$$\frac{E}{A} = Q_1 Q_2 Q_3 Q_4 \quad (33d)$$

This combination of roots appears to be non-physical.

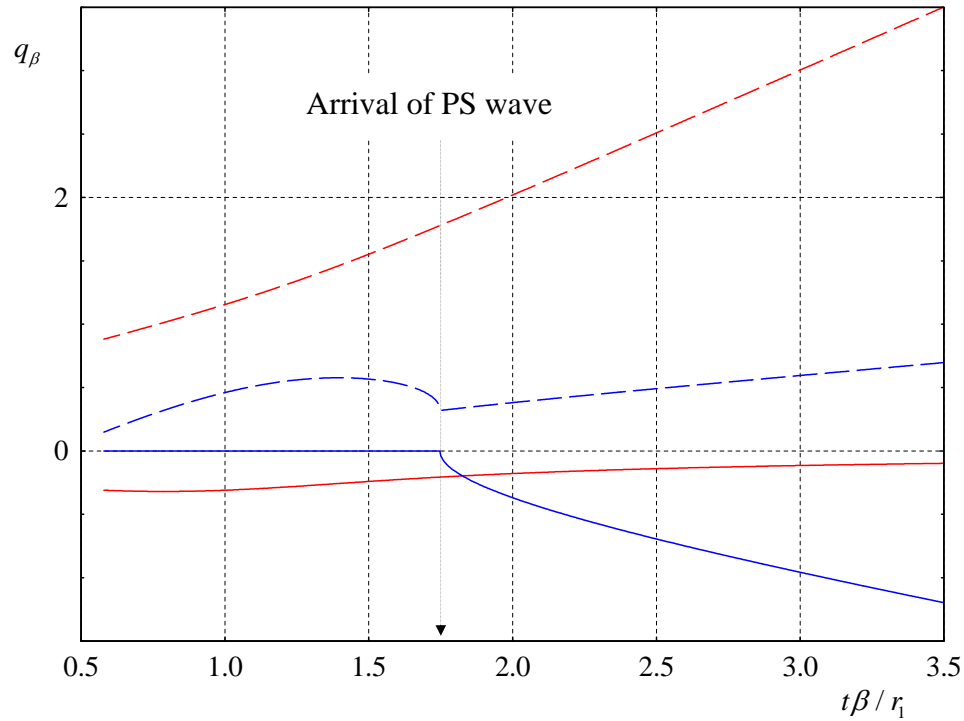
**Example:** Consider the source-receiver configuration  $h = x = z = 1$  together with the material parameters  $\beta = 1$ ,  $\nu = 0.25$ , which corresponds to Lamé constants  $\lambda = \mu = 1$ .

Figure 4a shows the two roots whose real part is positive, with one being unphysical, while Fig. 4b shows the other two unphysical roots whose real part is negative. Solid lines depict the real part while dashed lines display the imaginary part. For convenience, we choose to normalize the time axis with respect to  $r_1 = 1$ , which makes  $\tau_p = 1$ . Although we plot the four roots for an extended time interval, the true branch only comes into play

when  $t > t_{PS}$ . Observe that at all times there exists one pair of (negative) complex conjugate roots which is supplemented by another pair after the arrival of the PS wave. Before that time, the other two roots are purely imaginary, and they coalesce at  $t = t_{PS}$  (shown by an arrow).



**Figure 4a:** Roots of quartic with positive real part.  $t\beta/r_1$   
Real part = solid line, Imaginary part = dashed line



**Figure 4b:** Roots of quartic with negative real part.  
Real part = solid line, Imaginary part = dashed line

## Appendix 2: Matlab program

The Matlab program is provided in the ensuing. For a digital copy of this program, see the online version.

```
function Garvin2 (x,z,pois,h,Cs,rho)
% Solves the generalized Garvin problem of a line blast
% source applied at depth h within a homogeneous half-space.
% The response is sought within that same half-space
% at a receiver at range x and depth z.
%
% Written by Eduardo Kausel, MIT, Room 1-271, Cambridge, MA
% Version 1, July 19, 2011
%
% Input arguments:
%   x   = range of receiver >0
%   z   = depth of receiver >=0
%   pois = Poisson's ratio           Defaults to 0.25 if not given
%   h   = Depth of source   > 0      "      " 1 " " "
%   Cs  = Shear wave velocity        "      " 1 " " "
%   rho = mass density              "      " 1 " " "
%
% Sign convention:
%   x from left to right, z=0 at the surface, z points down
%   Displacements are positive down and to the right.
%
% References:
%   W.W. Garvin, Exact transient solution of the buried line source
%               problem, Proceedings of the Royal Society of London,
%               Series A, Vol. 234, No. 1199, March 1956, 528-541
%   Z.S. Alterman and D. Loewenthal, Algebraic Expressions for the
%               impulsive motion of an elastic half-space,
%               Israel Journal of Technology, Vol. 7, No. 6,
%               1969, pp. 495-504
%
% default data
if nargin<6, rho=1; end      % mass density
if nargin<5, Cs=1; end      % shear wave velocity
if nargin<4, h=1; end       % depth of source
if nargin<3, pois=0.25; end % Poisson's ratio
N = 1000; % number of time steps to arrival of PS waves

mu = rho*Cs^2; % shear modulus
r1 = sqrt(x^2+(z-h)^2); % source-receiver distance
r2 = sqrt(x^2+(z+h)^2); % image source-receiver distance
s1 = x/r1; % sin(theta1)
c1 = (z-h)/r1; % cos(theta1)
s2 = x/r2; % sin(theta2)
c2 = (h+z)/r2; % cos(theta2)

a2 = (0.5-pois)/(1-pois);
a = sqrt(a2); % Cs/Cp
Cp = Cs/a; % P-wave velocity
tS = r1/Cs; % S-wave arrival (none here)
tP = r1/Cp; % time of arrival of direct P waves
```

```

tPP = r2/Cp; % time of arrival of PP waves
tPS = t_PS (x,z,h,Cs,Cp); % time of arrival of PS waves
dt = (tPS-tP)/N; % time step
t1 = (tP+dt):dt:(tPP-dt); % time before reflections
t2 = (tPP+dt):dt:tPS; % time from PP to PS reflection
t3 = (tPS+dt):dt:3*tPS; % time after arrival of PS waves

% Find q3(tau) from tau(q3) by solving quartic
X=x/r2; Z=z/r2; H=h/r2;
A = ((H+Z)^2+X^2)*((H-Z)^2+X^2);
B1 = X*(X^2+H^2+Z^2);
C1 = X^2*(a2*H^2+Z^2)+(H^2-Z^2)*(a2*H^2-Z^2);
C2 = 3*X^2+H^2+Z^2;
D1 = X*(a2*H^2+Z^2);
E1 = (a*H+Z)^2;
E2 = (a*H-Z)^2;
tau = t3*Cs/r2; % dimensionless time for PS waves
q3 = [];
for j=1:length(t3)
    tau2 = tau(j)^2;
    B = tau(j)*B1;
    C = tau2*C2-C1;
    D = tau(j)*(tau2*X-D1);
    E = (tau2-E1)*(tau2-E2);
    q = roots([A,-4*i*B,-2*C,4*i*D,E]); % in lieu of Ferrari
    q = q(find(real(q)>=0 & imag(q)>=0)); % discard negative roots
    [q1,I] = min(imag(q)); % find position of true root
    q3 = [q3,q(I)]; % choose that root
end

% Sánchez-Sesma approximation:
%*****
R = (h+z/a)/(h+z); % r_eq/r2
r3 = R*r2; % equivalent radius
tapp = tau/R;
T = conj(sqrt(tapp.^2-a2)); % conj --> T must have neg. imag part
q3app = R*(c2*T+i*tapp*s2);
% Compare exact vs. approximate
plot(t3,real(q3));
hold on
plot(t3,imag(q3),'r');
plot(t3,real(q3app),'--');
plot(t3,imag(q3app),'r--');
grid on
title ('q3 --> exact vs. Sánchez-Sesma's approximation')
xlabel('Time')
pause
close

% Find and plot the time histories
% *****
% a) From tP to tPP
T1 = sqrt(t1.^2-tP^2);
f1 = (0.5/r1)*t1./T1;
u1 = f1*s1;
w1 = f1*c1;

```

```

% b) From tPP to tPS
T1 = sqrt(t2.^2-tP^2);
T2 = sqrt(t2.^2-tPP^2);
f1 = (0.5/r1)*t2./T1;
f2 = (0.5/r2)*t2./T2;
q2 = (c2*T2+i*s2*t2)*Cs/r2;
dq2 = c2*t2./T2+i*s2; % derivative
Q2 = q2.^2;
Q2S = sqrt(Q2+1);
Q2P = sqrt(Q2+a2);
S2 = (1+2*Q2).^2;
D2 = S2-4*Q2.*Q2S.*Q2P; % Rayleigh function
u2 = f1*s1-f2*s2-(4/r2)*imag(q2.^3.*Q2S.*dq2./D2);
w2 = f1*c1+f2*c2-(1/r2)*real(S2.*dq2./D2);

% c) From tPS and on
T1 = sqrt(t3.^2-tP^2);
T2 = sqrt(t3.^2-tPP^2);
f1 = (0.5/r1)*t3./T1;
f2 = (0.5/r2)*t3./T2;
% Contribution of PP waves
q2 = (c2*T2+i*s2*t3)*Cs/r2;
dq2 = c2*t3./T2+i*s2; % derivative
Q2 = q2.^2;
Q2S = sqrt(Q2+1);
Q2P = sqrt(Q2+a2);
S2 = (1+2*Q2).^2;
D2 = S2-4*Q2.*Q2S.*Q2P; % Rayleigh function
f3 = (4/r2)*imag(q2.^3.*Q2S.*dq2./D2);
f5 = (1/r2)*real(S2.*dq2./D2);
% Contribution of PS waves
Q3 = q3.^2;
Q3S = sqrt(Q3+1);
Q3P = sqrt(Q3+a2);
S = 1+2*Q3;
S3 = S.^2;
D3 = S3-4*Q3.*Q3S.*Q3P; % Rayleigh function
dq3 = 1./((h/r2./Q3P+z/r2./Q3S).*(q3-i*x/r2));
f4 = (2/r2)*imag(q3.*S.*Q3S.*dq3./D3);
f6 = (2/r2)*real(Q3.*S.*dq3./D3);
u3 = f1*s1-f2*s2-f3+f4;
w3 = f1*c1+f2*c2-f5+f6;

% Combine the results and plot
time = [[0,tP],t1,t2,t3]*Cs/r1;
u = [[0,0],u1,u2,u3]*(r1/pi);
w = [[0,0],w1,w2,w3]*(r1/pi);
plot(time,u);
tit = sprintf('Horizontal displacements at x =%f z =%f' , x, z);
title(tit);
xlabel('t*\beta/r1');
ylabel('Ux*r1*\mu');
grid on
pause
plot(time,w);
tit = sprintf('Vertical displacements at x =%f z =%f' , x, z);
title(tit);

```

```

xlabel('t*\beta/r1');
ylabel('Uz*r1*\mu');
grid on
pause
close
return

%-----
function [tPS,xP,xS] = t_PS (x,z,h,Cs,Cp)
% Determines the total travel time of the PS reflection
% Arguments
% *****
% x = range of receiver
% z = depth of receiver
% h = depth of source
% Cs = S-wave velocity
% Cp = P-wave velocity

if z==0, tPS=sqrt(x^2+h^2)/Cp; return; end
a = Cs/Cp;
% Bracket the S point
xP = x*h/(h+z); % point of reflection of PP ray
ang1 = atan(xP/h); % minimum angle of incident ray
ang2 = atan(x/h); % maximum angle
% Find the S point by search within bracket
dang = (ang2-ang1)/10;
TOL = 1.e-8;
TRUE = 1;
while TRUE
    angP = ang1+dang;
    angS = asin(a*sin(angP));
    L = h*tan(angP)+z*tan(angS);
    if L>x
        if L-x<TOL*x, break, else, dang = dang/10; end
    else
        ang1 = angP;
    end
end
tPS = h/cos(angP)/Cp+z/cos(angS)/Cs;
if nargout<3, return, end
xS = h*tan(angP); % point of reflection of PS ray
return

%-----
function [q] = Ferrari(A,B,C,D,E)
% Solves quartic equation
%  $Aq^4 - 4iBq^3 - 2Cq^2 + 4iDq + E$ 
% by Ferrari's method

B = B/A; C=C/A; D=D/A; E=E/A;
a = 2*(3*B^2-C);
b = 4*i*(D-B*C+2*B^3);
c = E-4*B*D+2*C*B^2-3*B^4;
if b==0
    s2 = sqrt(a^2-4*c);
    s1 = sqrt((s2-a)/2);
    s2 = sqrt((-s2-a)/2);

```

```

    q1 = i*B+s1;
    q2 = i*B-s1;
    q3 = i*B+s2;
    q4 = i*B-s2;
else
    P = -(a^2/12+c)/3;
    Q = a/6*(c-a^2/36)-b^2/16;
    R = sqrt(Q^2+P^3)-Q;
    U = R^(1/3);
    V = U-5/6*a;
    if U==0
        V = V-(2*Q)^(1/3);
    else
        V = V-P/U;
    end
    W = sqrt(a+2*V);
    s2 = -(3*a+2*V);
    s1 = sqrt(s2-2*b/W);
    s2 = sqrt(s2+2*b/W);
    q1 = i*B+0.5*(W-s1);
    q2 = i*B+0.5*(-W+s2);
    q3 = i*B+0.5*(W+s1);
    q4 = i*B+0.5*(-W-s2);
end
q = [q1, q2, q3, q4].';
return

```



## CORRIGENDUM

### Garvin's generalized problem revisited

by Francisco Sánchez-Sesma, Ursula Iturrarán Viveros, and Eduardo Kausel  
Soil Dynamics and Earthquake Engineering, Volume 47, April 2013, Pages 4-15

Equations 20a,20b in Section 3.4 providing the asymptotic (static) behavior at long times are incorrect, or more precisely, incomplete. This is the result of having neglected in our asymptotic expansion some higher-order terms which still contribute to the limiting value at infinite times. As it turns out, the exact derivation of those additional terms requires some rather substantial and sophisticated algebra, which would occupy considerable space in this journal. For this reason, we omit the details herein and merely provide the final results. The correct asymptotic expressions are:

$$u = \frac{1}{2\pi\mu} \left\{ \frac{1}{r_1} \sin\theta_1 + \frac{3-4\nu}{r_2} \sin\theta_2 - \frac{2}{r_2} \frac{z}{r_2} \sin 2\theta_2 \right\} \quad (20a)$$

$$w = \frac{1}{2\pi\mu} \left\{ \frac{1}{r_1} \cos\theta_1 - \frac{3-4\nu}{r_2} \cos\theta_2 - \frac{2}{r_2} \frac{z}{r_2} \cos 2\theta_2 \right\} \quad (20b)$$

We obtained these expressions first by direct formulation and evaluation of the static problem based on integral transform methods. Thereafter, a sophisticated (and lengthy) evaluation of the asymptotic expressions was obtained directly from the Garvin-Alterman-Loewenthal dynamic solution in our original paper by Prof. Paul Martin at the Colorado School of Mines, who kindly made it available to us. Delightfully, these expressions coincided perfectly.

The agreement of the two independent methods provides in turn a strong indication that the dynamic equations after Alterman and Loewenthal (eqs. 19a, 19b) are correct, because our first static, direct method made no use of that dynamic solution in the first place.